Characterising the atmospheric conditions leading to large error growth in volcanic ash cloud forecasts

Article

Accepted Version

To link to this article DOI: http://dx.doi.org/10.1175/jamc-d-17-0298.1

Publisher: American Meteorological Society

The DOI for this manuscript is doi: 10.1175/JAMC-D-17-0298.1

The final published version of this manuscript will replace the preliminary version at the above DOI once it is available.

If you would like to cite this EOR in a separate work, please use the following full citation:

Dacre, H., and N. Harvey, 2018: Characterising the atmospheric conditions leading to large error growth in volcanic ash cloud forecasts. J. Appl. Meteor. Climatol. doi:10.1175/JAMC-D-17-0298.1, in press.

Characterising the atmospheric conditions leading to large error growth in volcanic ash cloud forecasts

H.F.Dacre* and N.J.Harvey†

Department of Meteorology, University of Reading, Earley Gate, PO Box 243, Reading, RG6 6BB, United Kingdom

**Corresponding author address:* H.F.Dacre, Department of Meteorology, University of Reading, Earley Gate, PO Box 243, Reading, RG6 6BB, United Kingdom.

E-mail: h.f.dacre@reading.ac.uk

†Current affiliation: Department of Meteorology, University of Reading, Earley Gate, PO Box 243, Reading, RG6 6BB, United Kingdom.

ABSTRACT

Volcanic ash poses an ongoing risk to the safety of airspace worldwide. The accuracy to which we can forecast volcanic ash dispersion depends on the conditions of the atmosphere into which it is emitted. In this paper we use meteorological ensemble forecasts to drive a volcanic ash transport and dispersion model for the 2010 Eyjafjallajokull eruption. From analysis of these simulations we determine why the skill of deterministic-meteorological forecasts decrease with increasing ash residence time, and identify the atmospheric conditions in which this drop in skill occurs most rapidly. Large forecast errors are more likely when ash particles encounter regions of large horizontal flow separation in the atmosphere. Nearby ash particle trajectories can rapidly diverge leading to a reduction in the forecast accuracy of deterministic forecasts which do not represent variability in wind fields at the synoptic-scale. The flow separation diagnostic identifies where and why large ensemble spread may occur. This diagnostic can be used to alert forecasters to situations in which the ensemble mean is not representative of the individual ensemble member volcanic ash distributions. Knowledge of potential ensemble outliers can be used to assess confidence in the forecast and to avoid potentially dangerous situations in which forecasts fail to predict harmful levels of volcanic ash.

1. Introduction

Volcanic ash poses a significant hazard to aircraft. It can cause both temporary engine failure and permanent engine damage (*Guffanti et al.* 2005). Flights are therefore restricted in ash contaminated airspace, which disrupts air traffic leading to the potential for large financial loses. For example the 2010 Eyjafjallajökull eruption grounded over 95,000 flights, costing the airline industry over 1 billion pounds. Analysis of the 1900-2010 Icelandic historical records shows that a volcanic eruption of the size of the 2010 Eyjafjallajökull eruption has a repeat period of between 5 and 10 years (*Thordarson and Larson* 2007). Worldwide, volcanic eruptions 10 times the size of the 2010 Eyjafjallajökull eruption have repeat periods on a decadal timescale (e.g. Mount St Helens 1980, Hudson 1991, Puyehue 2011). Given the ongoing risk of volcanic eruptions it is important to continually evaluate and improve the accuracy of volcanic ash forecasts to ensure safe and optimised flight operations during future volcanic eruptions.

The volcanic ash advisory centres (VAACs) are responsible for producing volcanic ash cloud analysis and forecasts to assist the aviation community in planning their operations and minimising risks. There are currently 9 VAACs that together provide a comprehensive global modelling and warning system for the aviation community. These 9 VAACs use 6 different volcanic ash transport and dispersion (VATD) models to to produce volcanic ash charts showing the forecast location of volcanic ash in the atmosphere at different flight levels and out to forecast lead-times of 24 hours. VATD models are initialised using data about the location of the eruption, the time at which the eruption started and, if available, information about the plume rise height, vertical profile of volcanic ash and ash size distribution (known collectively as eruption source parameters, ESPs). They also use 3-D winds as input from numerical weather predictions to transport volcanic ash away from the source. Typically the meteorological input used has a horizontal resolution of between 10 and 50km. To represent dispersion on scales smaller than this horizontal diffusion is applied. The diffusion represents the dispersion by unresolved eddies and acts to increase the vertical and lateral spread of volcanic ash clouds (*Dacre et al.* 2015). This approach assumes that the small-scale dispersion processes are of an eddy viscosity character and thus can be represented using a Gaussian description (*Pasquill and Smith* 1983). The simulated ash cloud therefore represents the time mean of an ensemble of realisations.

At larger scales however, individual realisations can often display considerable deviations from the ensemble mean (*Mylne and Mason* 1991). The scale at which this occurs depends on the size of the dispersion processes relative to the width of the time averaged ash cloud. For averaging periods of a few hours, this scale is typically greater than 500 km. Variability on synoptic scales however differs for different atmospheric circulation patterns, meaning that the traditional Gaussian diffusion approach used for small-scale dispersion processes cannot be used. Current operational VATD models do not represent variability at the synoptic scale. They use meteorological input from a single realisation of the flow field to produce a volcanic ash forecast (referred to as *deterministic-met volcanic ash forecast* in this paper). The aim of this paper is to identify the atmospheric conditions in which there is a higher chance that deterministic-met volcanic ash forecast skill may rapidly decrease and to discuss the potential use of ensemble meteorological input to VATD models as a method to address the missing synoptic-scale variability in volcanic ash forecasts (referred to as *ensemble-met volcanic ash forecasts* in this paper).

Several studies have investigated the space and time-dependent skill of deterministic-met volcanic ash forecasts. For example, *Stunder et al.* (2007) analysed the forecast skill for 7 different volcanic eruptions by comparing deterministic-met volcanic ash forecasts with satellite observations. They showed that these forecasts were generally good for short-term (18 hours from start of the eruption) forecasts but that forecast skill appeared to decrease at longer lead-times. This relationship between volcanic ash forecast skill and forecast lead-time is due to (i) increasing errors in the forecast wind fields and ESPs at longer forecast lead-times and (ii) longer lead-time forecasts include particles with longer residence times. These particles experience an accumulation of errors in the wind field leading to larger positional errors on average than particles with shorter residence times. *Dacre et al.* (2016) examined the second of these sources of error by performing hindcast simulations of the Eyjafjallajökull eruption (using analysis wind fields). They showed that generally skill decreases as the residence time of ash increases but that the rate of skill decrease depends on the meteorological situation. In some situations only the position of ash particles with residence time less than 24 hours are correctly simulated whereas in other situations the position of ash particles with residence times longer than 72 hours can be accurately simulated. Other studies have shown that the inclusion of buffer zones, to account for positional errors in the deterministic-met volcanic ash clouds, can lead to significant improvement in the agreement with observations (*Webster et al.* 2012; *Grant et al.* 2012). These buffer zones are a simplistic attempt to account for uncertainty in the synoptic-scale wind fields.

For some time the use of ensemble-met volcanic ash forecasts has been advocated by the wider volcanic ash community (*Bonadonna et al.* 2012) as a more rigorous way of accounting for uncertainty in large-scale wind field. *Stefanescu et al.* (2014) and *Madankan et al.* (2014) include both ensemble meteorology and an ensemble of ESPs in their study to quantify overall uncertainty in volcanic ash forecasts. They demonstrate that the range of predicted concentrations can be large at forecast lead-times of 48 hours. Similarly *Vogel et al.* (2014) performed time-lagged ensemble simulations of volcanic ash dispersion from the Eyjafjallajökull plume and found that for some times the spread in ensemble-met forecasts is small but at others it is large. They attribute this to the nonlinear behaviour of the atmosphere. *Dare et al.* (2016) performed a comparison of both deterministic and ensemble-met volcanic ash forecasts for the 2014 Kelut eruption. They found that both showed good agreement with satellite observations for the first 12 hours from the start of the eruption. However, for longer lead-times (18-24 hours) the ensemble-met forecast showed better agreement with observations than the deterministic-met forecast.

While all these studies demonstrate that ensemble-met forecasts show better agreement with observations than the deterministic-met forecasts, particularly at longer lead-times, the dynamical reasons why they perform better has not been explored. The aim of our study therefore is to illustrate why the skill of deterministic-met forecasts decreases with increasing ash residence time, and furthermore to identify the atmospheric conditions in which this drop in skill occurs most rapidly. These conditions are identified using ECMWF meteorological ensembles as input to the NAME VATD model to simulate an ensemble of particle trajectories.

2. Methodology

a. Meteorological fields

In order to determine the uncertainty associated with the synoptic scale meteorological flow field an ensemble of meteorological forecasts are used. Each forecast is produced from perturbed initial conditions that represent the likely initial analysis error distribution. In this paper the European Centre for Medium Range Weather Forecasting (ECMWF) Integrated Forecasting System (cycle 41r1) has been used to create bespoke ensemble forecasts of the meteorological conditions during the 2010 eruption of Eyjafjallajökull. Global forecasts are initialised every 12 hours between 00 UTC on 1 May - 12 UTC on 8 May 2010. Each forecast is 42 hours long and has 20 ensemble members. Data is archived every 6 hours on 26 levels and at T639 spectral truncation (approximately 32km horizontal grid spacing). Initial perturbations are constructed using the singular-vector approach (*Buizza and Palmer* 1995) and model uncertainty is taken into account through the use of a simple stochastic physics scheme (*Buizza et al.* 1995). Data is extracted from the ECMWF archive at $0.25^\circ \times 0.25^\circ$ on a regular lat/lon grid and several fields (surface stresses, sensible heat flux and precipitation fields) are post-processed as data extracted from the ECMWF archive cannot be used directly as input to the VATD model described in section b.

b. NAME dispersion simulations

The VATD model used in this study is the Numerical Atmospheric-dispersion Modelling Environment (NAME). NAME is used by the London Volcanic Ash Advisory centre to forecast the spatial distribution of volcanic ash following an eruption. In this study we use NAME III (version 6.3) and ECMWF numerical weather prediction meteorological data to disperse particles released into the atmosphere at the position of the Eyjafjallajökull volcano in Iceland. The dispersion of volcanic ash by small-scale three-dimensional atmospheric turbulence and unresolved mesoscale motions are parametrized within NAME using random-walk techniques. The aim of the random-walk dispersion is to compute an ensemble of random trajectories of Lagrangian particles through a flow field whose statistics are based on observations of vertical and horizontal velocity variances and diffusivities (*Thomson and Wilson* 2013). The position of the particles is tracked for 42 hours to create particle trajectories. The volcanic ash density is assumed to be $2300\,\mathrm{kg\ m^{-3}}$ based on the value used in the operational version of NAME (*Leadbetter and Hort* 2011) and the particle size is assumed to be $2\,\mu\mathrm{m}$ based on in-situ observations of the ash cloud by the FAAM aircraft over and around the UK in the Eyjafjallajokull ash cloud (*Johnson et al.* 2012). Particles are subject to removal processes including sedimentation, wet and dry deposition (*Jones et al.* 2007). Note that the choice of particle size does not affect the conclusions reached in the paper.

c. SEVIRI satellite observations

To qualitatively evaluate the performance of the NAME forecasts we compare simulated ash cloud distributions with data from the Spinning Enhanced Visible and Infrared imager (SEVIRI). SEVIRI volcanic ash retrievals are calculated using brightness temperature difference measurements (see *Francis et al.* (2012) for more details). The advantage of using volcanic ash retrievals from an instrument onboard a geostationary satellite is that they are available at high temporal resolution, every hour, allowing us to track the evolution of the volcanic ash cloud and to interpolate between timesteps when water or ice clouds obscure the volcanic ash. Following the method of *Harvey and Dacre* (2016) we composite satellite observations over a 5 hour time window. This has been shown to be sufficient to create a continuous time series while remaining highly correlated with the noncompostied fields. The satellite volcanic ash retrievals are averaged onto a $0.5° \times 0.5°$ latitude/longitude grid to allow direct comparison with the NAME output.

d. Ensemble spread and flow separation diagnostics

One measure of the uncertainty in meteorological flow conditions is the time evolution of spatial spread in particle trajectories. In this paper the ensemble spread is calculated using the root-mean-square (*RMS*) distance between individual ensemble particle positions (1 particle from each ensemble simulation), ($\mathbf{x}_i$), and the mean position of the particles, ($\bar{\mathbf{x}}_i$), summed over all N particles (thus N equals 20 as there are 20 ensemble simulations). The distance is measured perpendicular to the mean direction travelled by the particles during the previous 10 minutes to capture lateral spreading of the trajectories only.

$$RMS = \sqrt{\frac{1}{N}\sum_{i}^{N}(\mathbf{x}_i - \bar{\mathbf{x}}_i)^2} \quad (1)$$

The diagnostic used to characterise the synoptic-scale flow conditions is the 2-D horizontal flow separation diagnostic introduced in *Dacre et al.* (2016). This flow separation is calculated as the velocity gradient perpendicular to the flow.

$$\frac{\partial \mathbf{v}}{\partial n} = \frac{1}{q^2}\left[v^2\frac{\partial u}{\partial x} - uv\left(\frac{\partial u}{\partial y} + \frac{\partial v}{\partial x}\right) + u^2\frac{\partial v}{\partial y}\right] \tag{2}$$

where **v** is the velocity vector, q is the wind speed, n is distance in the direction perpendicular to the flow, and x and y are distances in longitude and latitude directions, respectively. Where this diagnostic is positive, the atmospheric flow separates, and where it is negative, the flow contracts. Thus it is a good diagnostic for identifying where particle trajectories will spread apart. The flow separation diagnostic is related to the 3-D Lyapunov exponents used by *Legras et al.* (2005) and *Pisso and Legras* (2008) to characterise the rate of separation of infinitesimally close trajectories in phase space.

3. Results

a. Satellite-detected ash clouds

Figure 1(a) and (b) show the ash cloud from the Eyjafjallajökull eruption, as detected by the SEVIRI instrument. At 12 UTC on 7 May (figure 1(a)) the ash was detected in a coherent plume extending southward from Iceland to the west of the UK. The ash cloud exhibits an anticyclonic curvature as ash particles were transported anticyclonically around a high-pressure centre in the North-Atlantic. At around 50°N the ash cloud has started to bifurcate with one branch of volcanic ash continuing to follow an anticyclonic trajectory whilst another branch was advected cyclonically towards southern Europe. This cyclonic branch reaches the coast of Portugal at 00 UTC on the 8 May (figure 1(b)) whilst the majority of the volcanic ash continues to travel anticyclonically. The ability of VATD models to capture this complex ash cloud bifurcation is dependent on the accurate representation of the input meteorological wind fields. For example, *Wilkins et al.* (2016) showed that their NAME deterministic-met volcanic ash forecast was not able to capture the structure the thin filament of ash extending over northern Spain on 8 May 2010.

b. Ensemble member forecasts

Figures 1(c),(d) and (e),(f) show two volcanic ash forecasts using different ECMWF ensemble member flow fields, both initialised at 00 UTC on 6 May 2010. Particles are released at the location of Eyjafjallajökull volcano at a rate of 3600/hr. All of the particles were released at a height consistent with the maximum observed plume height at that time. It can be seen that close to the volcano the volcanic ash distribution for both forecasts is very similar, with both forecasts producing an ash cloud extending southward from Iceland to the west of the UK, consistent with the satellite detected ash cloud location. However, at 50°N the forecasts start to diverge. In figures 1(e) and (f) the majority of the volcanic ash is transported cyclonically and is advected towards Europe. In contrast in figures 1(c) and (d) the majority of the volcanic ash cloud continues to travel anticyclonically and is advected into the North Atlantic. For this example, the deterministic-met forecast shown in figures 1(c) and (d) would be considered a good forecast as it closely matches the evolution of the ash cloud seen in the satellite observations. However the deterministic-met forecast shown in figures 1(e) and (f) would be considered a poor forecast as it does not forecast the observed ash in the North Atlantic. This is despite both forecasts using equally plausible realisations of the flow field. This example highlights the danger of using a single deterministic-met flow field as input to a VATD model to forecast the ash cloud distribution. These 2 ensemble members are chosen because they exhibit very different volcanic ash cloud evolutions, the other 18 ensemble members result in ash distributions which resemble a mixture of the two extremes.

c. Flow separation

In this section we explain why the ensemble member forecasts differ so much from each other. In order to do this we examine the flow pattern at approximately 50°N and 15°W, the location at which the ash particle trajectories show an increase in spread.

Figures 2(a) and (b) shows the streamlines and flow separation at 12UTC and 18UTC on 6 May respectively, for a single deterministic-met ensemble member forecast. The streamlines evolve over time but broadly show a low pressure to the west of the domain, a large region of high pressure in the centre of the domain and low pressure in the east of the domain. Figures 2(a) and (b) also show the flow separation diagnostic averaged over 100hPa at the release height of the ash particles. The flow separation is positive in regions where the streamlines spread apart and negative where the streamlines contract. For the purposes of illustrating why different ensemble members diverge and under what conditions, it is not feasible to visualise the trajectories of thousands of particles. Therefore, for simplicity, we have chosen to visualise a single particle trajectory (that is not subject to stochastic motions) from each ensemble member. The thick black trajectory shown in figures 2(a) and (b) is a single 42 hr particle trajectory from the same ensemble simulation shown in figure 1(e) and (f)). This particle was released from the volcano source at 06 UTC and is subject to the flow field shown in figures 2(a) and (b). In order to isolate transport by the resolved-scale flow it is not subject to perturbations representing unresolved eddies, hence its smooth trajectory. The black star indicates the location of the particle at the time of the flow separation field. 12 hours after the particle is released into the atmosphere (figure 2(a)) the particle is at 57°N, 13°W where the streamlines are roughly parallel to one another and hence flow separation is small. 24 hours after the particle is released into the atmosphere (figure 2(b)) the particle is at 51°N, 17°W and is in a region of strong positive flow separation. The streamlines spread apart as they approach the point of intersection between the trough and ridge region (known as a col or saddle point).

It is difficult to analyse the along-trajectory flow separation in this Eulerian framework, therefore figure 2(c) shows the flow separation extracted at the relevant time along the Lagrangian particle trajectory. This Lagrangian analysis demonstrates that the particle advected in this deterministic-met forecast enters a region of strong flow separation at 52°N, 17°W. In order to determine whether this is specific to a single ensemble-met member forecast or to all of the meteorological ensemble forecasts initialised at 06UTC on 6 May the along-trajectory flow separation has been calculated for each of the meteorological ensemble forecast members. Figure 2(d) shows the evolution of flow separation along 20 particle trajectories released at the same time, a single particle trajectory in each ensemble-met forecast. The flow separation in each ensemble-met forecast is very similar up until the point at which the trajectories start to diverge. This is expected since the regions of positive and negative flow separation are spatially coherent. It also illustrates how the trajectory separation rapidly increases after the point at which the trajectories encounter the region of positive flow separation. Performing an ensemble-met volcanic ash forecast for this case accounts for the variability in the synoptic flow field and is necessary to fully encompass the ash cloud distribution uncertainty due to the flow field.

d. Trajectory spread

To establish if trajectory spreading always rapidly increases after trajectories encounter regions of positive flow separation similar experiments were performed for meteorological ensemble forecasts initialised at 06UTC on the 15 April - 7 May 2010. For each of these ensemble forecasts a single particle were released at a height corresponding to the observed plume top from the Eyjafjallajökull volcano. It is well known that in low wind-speed conditions wind direction can vary significantly in a short period of time causing particle trajectories can rapidly diverge (*Venkatram et al.* 2004). In this paper we choose to focus on the less well studied uncertainty occurring in moderate-strong wind conditions and thus only analyse the situations in which the wind speed at the release height was greater than 10m s^{-1}. Figure 3 shows the ensemble-met member forecasts with the 4 highest (figures 3(a)-(d)) and 4 lowest (figures 3(e)-(h)) trajectory spreads. Individual particle trajectories correspond to a single particle released at the same time in each ensemble-met member forecast. It can be seen that on some days, figures 3(a)-(d), the trajectories diverge after encountering regions of positive flow separation, consistent with the analysis for the 6 May 2010 (figures 2(d)). By comparison on other days, figures 3(e)-(h) the trajectories remain close together for 42 hours.

Figure 4 quantitatively describes the relationship between residence time and ensemble-met forecast trajectory spread (measured using the RMS perpendicular distance described in section d). As observed in figure 3 trajectory spread generally increases with residence time but not always at the same rate. The rate of trajectory spread depends on the synoptic situation. Figure 4 also shows the maximum along-trajectory flow separation from each ensemble-met forecast, accumulated over 42 hours for each set of simulations. The simulation with the smallest trajectory spread after 42 hours residence time corresponds to the 3 May 2010 (figure 3(h)) and the along-trajectory accumulated flow separation is small at all points along the trajectory. By contrast the simulation with the largest trajectory spread corresponds to the 19 April 2010 (figure 3(a)) and the along-trajectory accumulated flow separation is neutral or positive at all points along the trajectory. Thus, these simulations suggest that trajectories that experience large along-trajectory accumulated flow separation are more likely to spread apart than trajectories that experience no large along-trajectory flow separation, potentially leading to large error growth for a single deterministic forecast (as shown in figure 1)

4. Discussion and Conclusions

In this paper we examine the atmospheric flow characteristics that lead to volcanic ash cloud bifurcation and a reduction in forecast skill. We performed multiple forecasts using the UK Met Office volcanic ash transport and dispersion model (NAME) and input from ensemble meteorological flow fields from the ECMWF ensemble prediction system.

In moderate to strong wind situations the atmospheric conditions leading to large variability in volcanic ash particle positions are associated with large flow separation. When ash particles encounter regions of large horizontal flow separation their future trajectories are very sensitive to their position at that time. Nearby ash particle trajectories can rapidly diverge leading to a reduction in forecast accuracy for deterministic-met volcanic ash forecasts. Potentially leading to predictions of ash-free airspace in regions that are in-reality contaminated with ash or vice versa.

In order to fully represent the synoptic-scale meteorological uncertainty ensemble-met volcanic ash forecasts are needed. When volcanic ash clouds encounter regions of large flow separation the individual ensemble-met members may display considerable deviations from the ensemble mean. 2-D fields of positive flow separation could be used as a flag to alert forecasters to this potential risk and the individual ensemble-met member forecasts analysed. A combination of the flow separation diagnostic and ensemble volcanic ash forecasts will help to identify where and why large uncertainty in the forecast occurs and provide an estimate of the confidence of the forecast. For example, a forecaster could reduce the size of the hazardous area whenever high confidence in the ash cloud forecast was indicated. Reductions in the hazard area would avoid unnecessary disruption to airspace.

In this paper we have only considered the uncertainty in the horizontal wind fields. Uncertainty also exists in the magnitude and location of precipitation which leads to wet-deposition of volcanic ash. This uncertainty may also cause large errors in the magnitude of volcanic ash forecasts as precipitation is a very efficient removal mechanism. We have also not considered the uncertainty associated with the volcanic eruption source parameters (ESPs). The best way to combine the meteorological and ESP uncertainty and effective ways of communicating this uncertainty with users is the subject of future work.

Acknowledgments. We are grateful to Pete Francis and Mike Cooke at the UK Met Office for making their satellite derived volcanic ash data available. We also acknowledge use of ECMWF's computing and archive facilities. Natalie Harvey gratefully acknowledges funding from NERC grant NE/J017221/1 Probability, Uncertainty and Risk in the Environment. We thank Andrew Jones at the UK Met Office for his help in performing the NAME ensemble simulations and Alan Grant and Peter Clark for useful discussions on this work. The SEVIRI satellite data and NAME simulation output are available in University of Reading Research Data Archive, http://dx.doi.org/10.5072/uor-data-00000000. Further information about the data supporting these findings and requests for access to the data can be directed to h.f.dacre@reading.ac.uk.

References

References

Bonadonna, C., Folch, A., Loughlin, S. and Puempel, H., (2012). Future developments in modelling and monitoring of volcanic ash clouds: outcomes from the first IAVCEI-WMO workshop on Ash Dispersal Forecast and Civil Aviation. *Bulletin of volcanology 74*, 1-10.

Buizza, R. and Palmer, T.N., (1995). The singular-vector structure of the atmospheric global circulation. *Journal of the Atmospheric Sciences 52*, 1434-1456.

Buizza, R., Milleer, M. and Palmer, T.N., (1999). Stochastic representation of model uncertainties in the ECMWF ensemble prediction system. *Quarterly Journal of the Royal Meteorological Society 125*, 2887-2908.

Dacre, H.F., Harvey, N.J., Webley, P.W. and Morton, D., (2016). How accurate are volcanic ash simulations of the 2010 Eyjafjallajökull eruption? *Journal of Geophysical Research: Atmospheres 121*, 3534-3547.

Dacre, H.F., Grant, A.L.M., Harvey, N.J., Thomson, D.J., Webster, H.N. and Marenco, F., (2015). Volcanic ash layer depth: Processes and mechanisms. *Geophysical Research Letters 42*, 637-645.

Dare, R.A., Smith, D.H. and Naughton, M.J., (2016). Ensemble Prediction of the Dispersion of Volcanic Ash from the 13 February 2014 Eruption of Kelut, Indonesia. *Journal of Applied Meteorology and Climatology 55*, 61-78.

Francis, P. N., M. C. Cooke, and R. W. Saunders (2012). Retrieval of physical properties of volcanic ash using Meteosat: A case study from the 2010 Eyjafjallajökull eruption. *Journal of Geophysical Research*, *117*, D20, doi:10.1029/2011JD016788.

Grant, A.L., Dacre, H.F., Thomson, D.J. and Marenco, F., (2012). Horizontal and vertical structure of the Eyjafjallajökull ash cloud over the UK: a comparison of airborne lidar observations and simulations. *Atmospheric Chemistry and Physics 12*, 10145-10159.

Guffanti, M., Ewert, J.W., Gallina, G.M., Bluth, G.J. and Swanson, G.L., (2005). Volcanic-ash hazard to aviation during the 2003-2004 eruptive activity of Anatahan volcano, Commonwealth of the Northern Mariana Islands. *Journal of Volcanology and Geothermal Research 146*, 241-255.

Harvey, N. J. and Dacre, H. F. (2016). Spatial evaluation of volcanic ash forecasts using satellite observations (2016)*Atmos. Chem. Phys. 16*, 861-872.

Johnson, B., Turnbull, K., Brown, P., Burgess, R., Dorsey, J., Baran, A.J., Webster, H., Haywood, J., Cotton, R., Ulanowski, Z. and Hesse, E., (2012). In situ observations of volcanic ash clouds from the FAAM aircraft during the eruption of Eyjafjallajkull in 2010. *Journal of Geophysical Research: Atmospheres*, *117*, D20.

Jones, A., Thomson, D., Hort, M. and Devenish, B., (2007). The UK Met Office's next-generation atmospheric dispersion model, NAME III *Air Pollution Modeling and its Application XVII*, 580-589. Springer US.

Leadbetter, S.J. and Hort, M.C., (2011). Volcanic ash hazard climatology for an eruption of Hekla Volcano, Iceland. *Journal of Volcanology and Geothermal Research*, *199*, 230-241.

Legras, B., Pisso, I., Lefevre, F., and Berthet, G. (2005). Lagrangian turbulent diffusion in the lower stratosphere Atmos.Chem. Phys., *5*, 1605-1622.

Madankan, R., Pouget, S., Singla, P., Bursik, M., Dehn, J., Jones, M., Patra, A., Pavolonis, M., Pitman, E.B., Singh, T. and Webley, P., (2014). Computation of probabilistic hazard maps and source parameter estimation for volcanic ash transport and dispersion. *Journal of Computational Physics 271*, 39-59.

Mylne, K.R. and Mason, P.J., (1991). Concentration fluctuation measurements in a dispersing plume at a range of up to 1000 m. *Quarterly Journal of the Royal Meteorological Society*, *117*, 177-206.

Pasquill F. and Smith, F. B. (1983). *Atmospheric Diffusion*, thrid edition, Ellis Horwood, Chichester.

Pisso, I. and Legras, B. (2008). Turbulent vertical diffusivity in the sub-tropical stratosphere *Atmos. Chem. Phys.*, *8*, 697-707.

Stefanescu, E. R., Patra, A. K, Bursik, M. I., Madankan, R., Pouget, S., Jones, M., Singla, P., Singh, T., Pitman, E. B., Pavolonis, M., Morton, D., Webley, P. and Dehn, J. (2014). Temporal, probabilistic mapping of ash clouds using wind field stochastic variability and uncertain eruption source parameters: Example of the 14 April 2010 Eyjafjallajökull eruption. *J. Adv. Model. Earth Syst 6*, 1173-1184, doi:10.1002/2014MS000332.

Stunder, B.J., Heffter, J.L. and Draxler, R.R. (2007), Airborne volcanic ash forecast area reliability. *Weather and Forecasting 22*, 1132-1139.

Thomson, D.J. and Wilson, J.D., (2013). History of Lagrangian stochastic models for turbulent dispersion. *Lagrangian modelling of the atmosphere, Geophysical Monograph Series 200, American Geophysical Union*, 19-36.

Thordarson, T. and Larsen, G. (2007), Volcanism in Iceland in historical time: Volcano types, eruption styles and eruptive history. *Journal of Geodynamics 43*, 118-152.

Webster, H. N., Thomson, D. J., Johnson, B. T., Heard, I. P. C., Turnbull, K., Marenco, F., Kristiansen, N. I., Dorsey, J., Minikin, A., Weinzierl, B., Schumann, U., Sparks, R. S. J., Loughlin, S. C., Hort, M. C., Leadbetter, S. J., Devenish, B. J., Manning, A. J., Witham, C. S., Haywood, J. M., and Golding, B. W. (2012), Operational prediction of ash concentrations in the distal volcanic cloud from the 2010 Eyjafjallajökull eruption, *J. Geophys. Res. 117*, DOI:10.1029/2011JD016790.

Venkatram, A., Isakov, V., Yuan, J., and Pankratz, D. (2004). Modeling dispersion at distances of meters from urban sources.*Atmospheric Environment 38*, 4633-4641.

Vogel, H., Förstner, J., Vogel, B., Hanisch, T., Mühr, B., Schättler, U. and Schad, T. (2014). Time-lagged ensemble simulations of the dispersion of the Eyjafjallajökull plume over Europe with COSMO-ART.*Atmospheric Chemistry and Physics 14*, 7837-7845.

Wilkins, K. L., I. M. Watson, N. I. Kristiansen, H. N. Webster, D. J. Thomson, H. F. Dacre and A. J. Prata (2016). Using data insertion with the NAME model to simulate the 8 May 2010 Eyjafjallajökull volcanic ash cloud, *Journal of Geophysical Research*, *121*, doi:10.1002/2015JD023895.

LIST OF FIGURES

Fig. 1. 5 hour composite of satellite-detected ash clouds at (a) 12 UTC on 7 May, (b) 00 UTC on 8 May 2010. (c)-(f) show ash column loading forecasts for two ensemble member forecasts both initialised at 06 UTC on 6 May 2010. (c),(e) valid at 12 UTC on 7 May, (d),(f) valid at 00 UTC on 8 May 2010 21

Fig. 2. Flow separation averaged from 325-225hPa (filled contours) overlaid with 275hPa streamlines (grey) at (a) 18TUC on 6 May 2010, and (b) 06 UTC on 7 May 2010. 42hr particle trajectory initialised at 06 UTC on 6 May 2010 (thick black line) and position of particle at time of flow separation and streamline fields (black star). (c) Flow separation along the particle trajectory shown in (a) and (b) from 12 hrs residence time onwards. (d) Flow separation along 20 particle trajectories advected by 20 different forecast wind fields. 22

Fig. 3. Ash particle trajectories for 42 hour forecasts with perturbed initial conditions. Forecasts with the highest trajectory spread after 42 hours (a)-(d) and lowest trajectory spread after 42 hours (e)-(h). Colours show 6-hourly averaged flow separation. 23

Fig. 4. Evolution of ensemble spread for 14 simulations initialised at 06UTC between 15 April and 7 May 2010. Colours show the along-trajectory accumulated maximum flow separation. 24

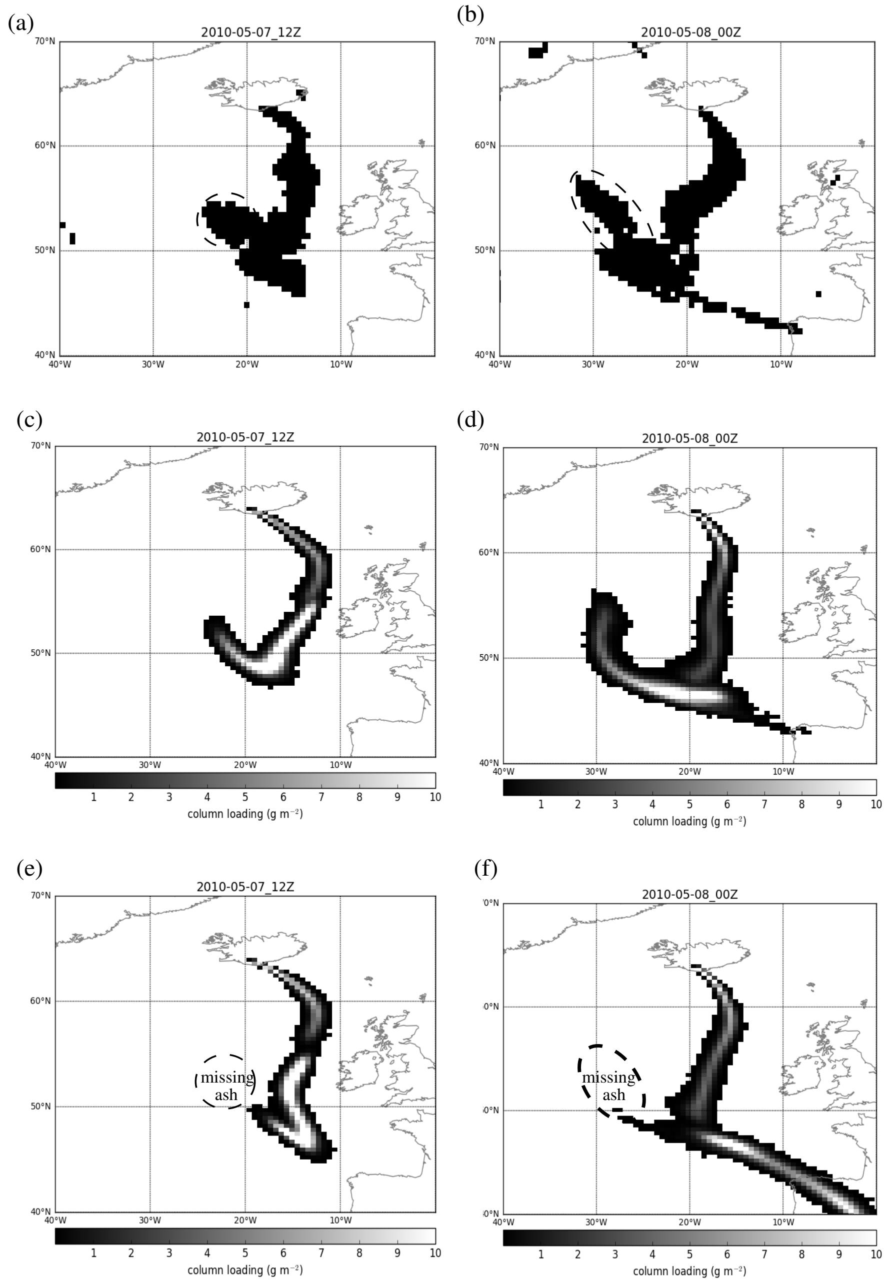

FIG. 1. 5 hour composite of satellite-detected ash clouds at (a) 12 UTC on 7 May, (b) 00 UTC on 8 May 2010. (c)-(f) show ash column loading forecasts for two ensemble member forecasts both initialised at 06 UTC on 6 May 2010. (c),(e) valid at 12 UTC on 7 May, (d),(f) valid at 00 UTC on 8 May 2010

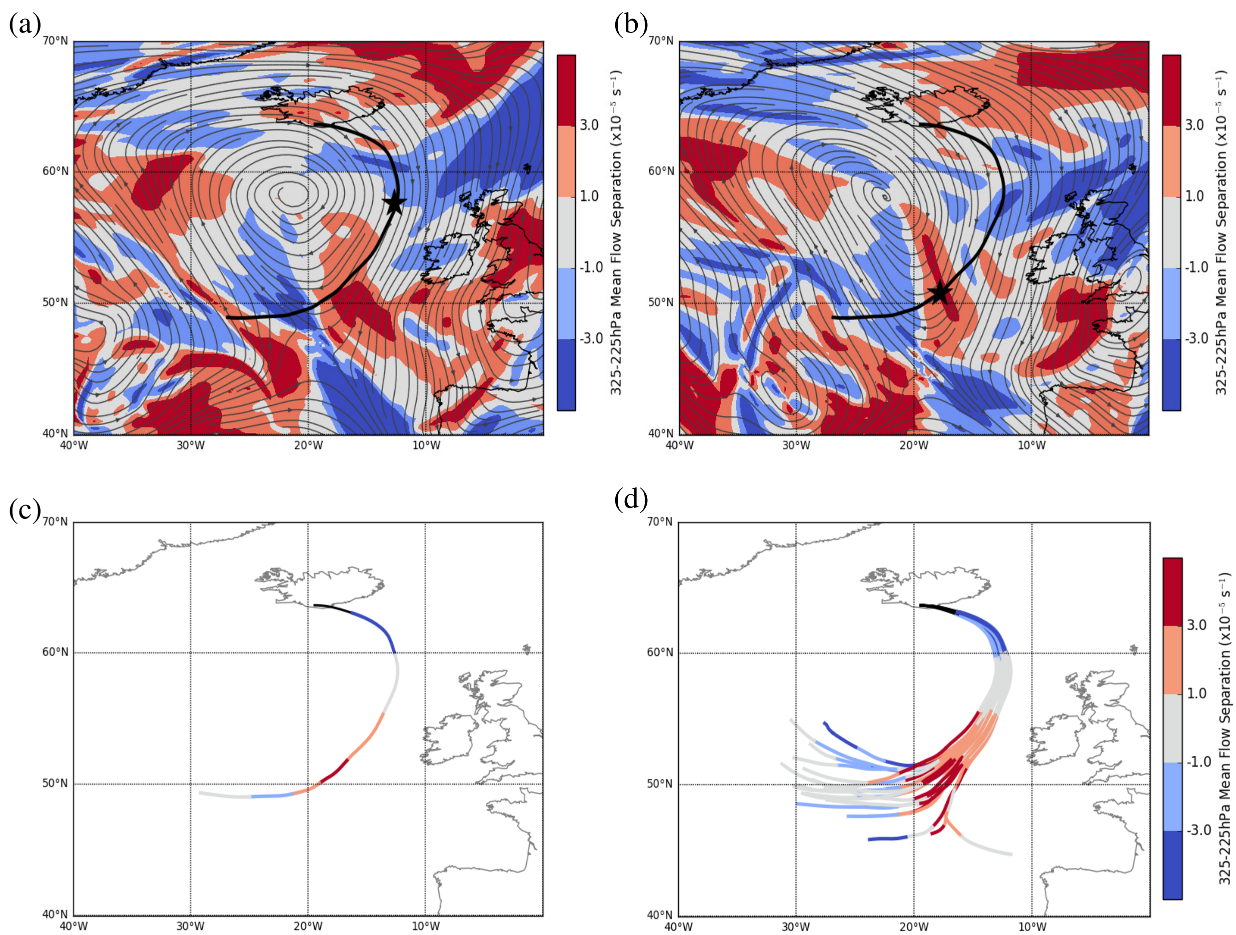

FIG. 2. Flow separation averaged from 325-225hPa (filled contours) overlaid with 275hPa streamlines (grey) at (a) 18TUC on 6 May 2010, and (b) 06 UTC on 7 May 2010. 42hr particle trajectory initialised at 06 UTC on 6 May 2010 (thick black line) and position of particle at time of flow separation and streamline fields (black star). (c) Flow separation along the particle trajectory shown in (a) and (b) from 12 hrs residence time onwards. (d) Flow separation along 20 particle trajectories advected by 20 different forecast wind fields.

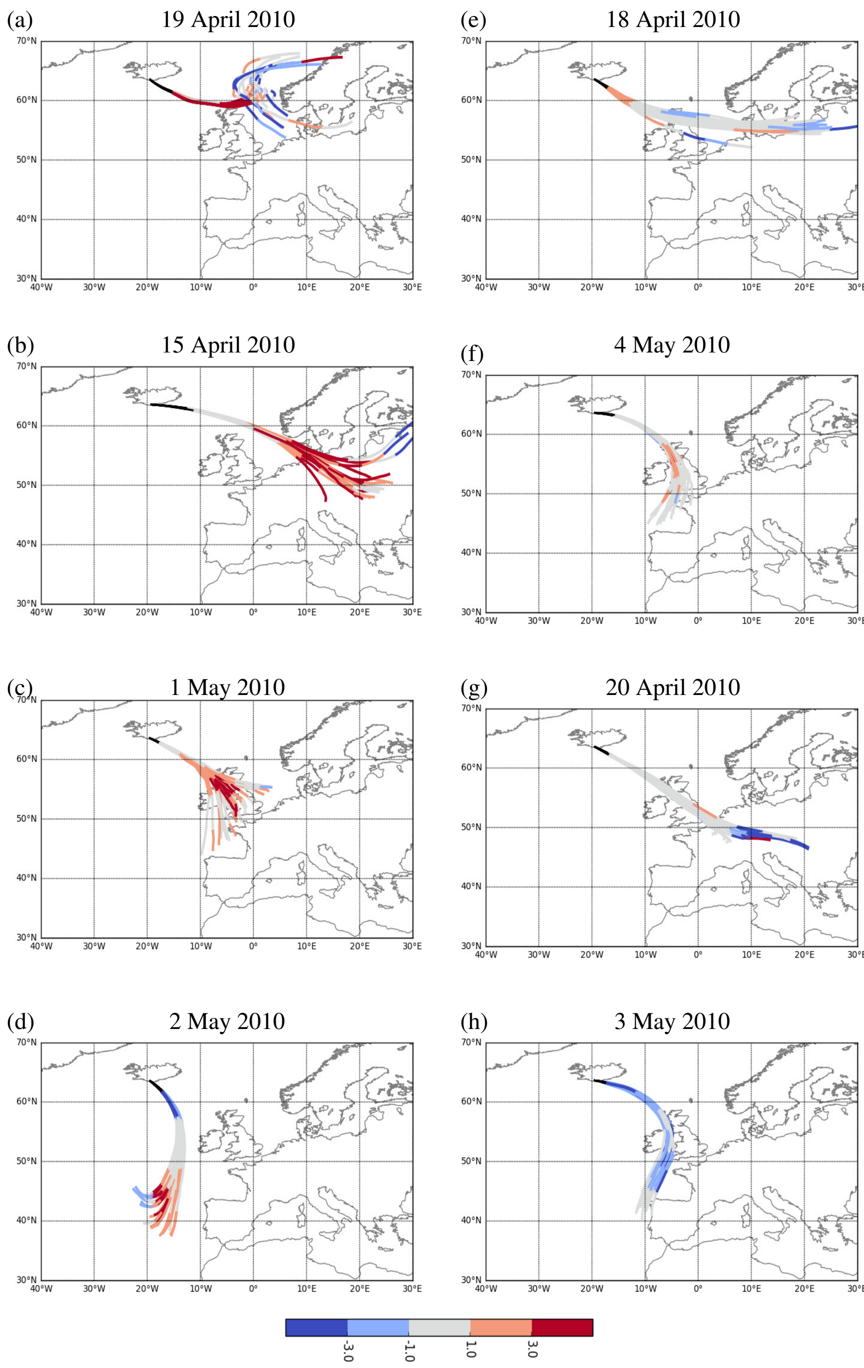

FIG. 3. Ash particle trajectories for 42 hour forecasts with perturbed initial conditions. Forecasts with the highest trajectory spread after 42 hours (a)-(d) and lowest trajectory spread after 42 hours (e)-(h). Colours show 6-hourly averaged flow separation.

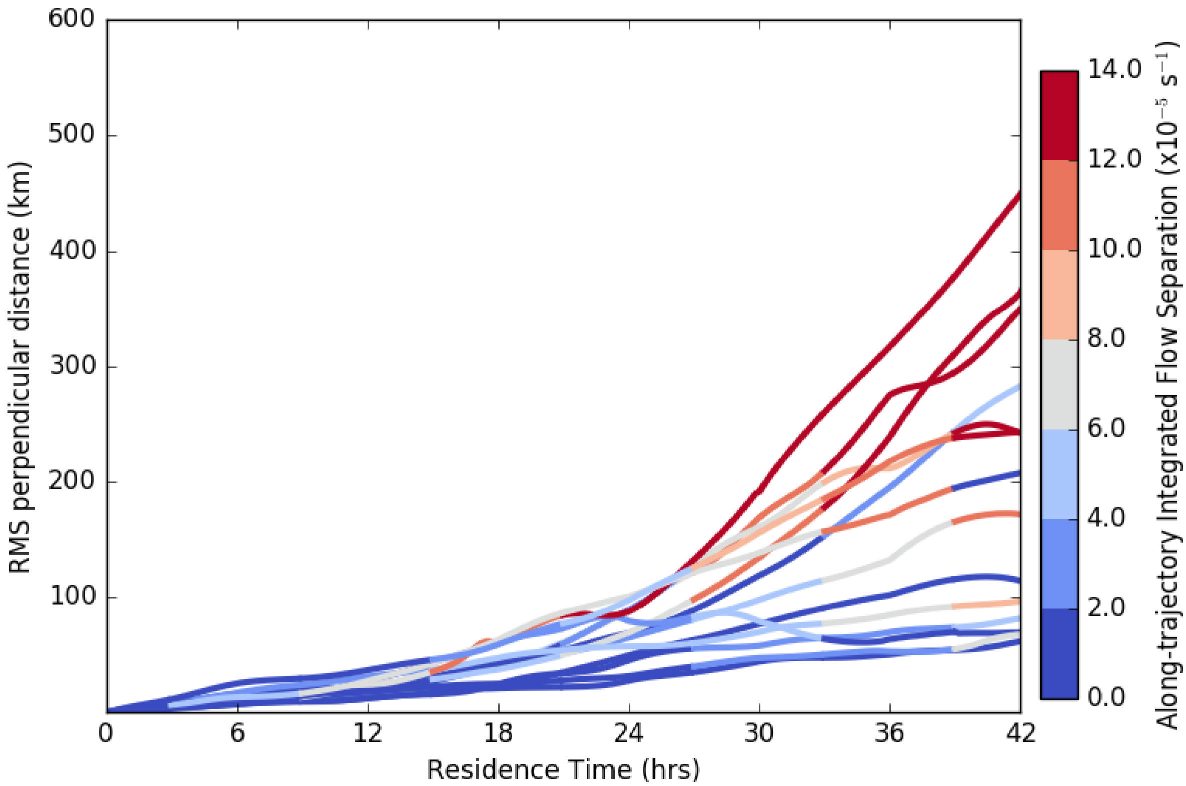

FIG. 4. Evolution of ensemble spread for 14 simulations initialised at 06UTC between 15 April and 7 May 2010. Colours show the along-trajectory accumulated maximum flow separation.